

---

# Procedures for Three-Dimensional Reconstruction of Spherical Viruses by Fourier Synthesis from Electron Micrographs

R. A. Crowther

*Phil. Trans. R. Soc. Lond. B* 1971 **261**, 221-230  
doi: 10.1098/rstb.1971.0054

---

## References

Article cited in:

<http://rstb.royalsocietypublishing.org/content/261/837/221#related-urls>

## Email alerting service

Receive free email alerts when new articles cite this article - sign up in the box at the top right-hand corner of the article or click [here](#)

---

To subscribe to *Phil. Trans. R. Soc. Lond. B* go to: <http://rstb.royalsocietypublishing.org/subscriptions>

---

## Procedures for three-dimensional reconstruction of spherical viruses by Fourier synthesis from electron micrographs

BY R. A. CROWTHER

*Medical Research Council, Laboratory of Molecular Biology, Hills Road, Cambridge*

[Plates 43 and 44]

An account is given of a method which has been developed for computing three-dimensional density maps from transmission electron micrographs using Fourier transforms. The reconstructions objectively combine data from several different views of one or more particles. The application to negatively stained tomato bushy stunt virus is described in detail and the resulting reconstruction presented. Projections of the reconstruction in the appropriate directions agree well with images of the virus taken from micrographs.

### 1. INTRODUCTION

Conventional electron microscopes possess a large depth of focus. Consequently a transmission electron micrograph represents a projection of the scattering density in the specimen onto a plane normal to the direction of the electron beam. Knowledge of three-dimensional relationships between the various parts of the specimen must therefore be obtained from one or more of these projected views of the object. A general method involving the use of Fourier transforms has been proposed (DeRosier & Klug 1968). It has been applied (DeRosier & Klug 1968; Moore, Huxley & DeRosier 1970; Finch & Gibbs 1970) to biological assemblies with helical symmetry, for which special case a single view of the particle may provide sufficient information to reconstruct the object at least to limited resolution, since the two-dimensional transform obtained directly from one image can be used in a Fourier–Bessel inversion. For non-helical particles it is necessary to combine data from a number of different projected views and this, in turn, requires data reduction and interpolation (Crowther, DeRosier & Klug 1970). We have developed mathematical and computational procedures for implementing the method and have applied these to reconstructions of spherical viruses, where a number of different views are required. A brief account of this work has been given by Crowther, Amos, Finch, DeRosier & Klug (1970). In this paper we describe in detail the actual procedures used.

In spherical viruses the coat protein molecules are arranged with icosahedral symmetry (Caspar & Klug 1962) to form a protective covering for the nucleic acid. This kind of particle is well preserved in negatively stained preparations, and the high symmetry and possibility of recognizing the orientation of certain special views make it a natural choice for testing the extended system of reconstruction. Above all, the presence of high symmetry means that in principle only a small number of distinct views are required for their reconstruction.

We now describe the method and then discuss its application to tomato bushy stunt virus.

### 2. THE METHOD OF RECONSTRUCTION

The method of reconstruction is based on the projection theorem, which states that the two-dimensional Fourier transform of a plane projection of a three-dimensional density distribution is identical with the corresponding central section of the three-dimensional transform normal to the direction of view. The three-dimensional transform can therefore be built up section by

section using transforms of different views of the object, and the three-dimensional reconstruction then produced by Fourier inversion. The approach is similar to conventional X-ray crystallography, except that the phases of the X-ray diffraction pattern cannot be measured directly, whereas in electron microscopy they can be computed from an image.

The different views may be collected either from a single particle by using a tilting stage in the microscope, or from a number of particles in different but identifiable orientations. In general, it is desirable to combine data from different particles so that imperfections can be averaged out. When different particles are viewed from different angles their absolute orientation must first be found; we have developed a method for identifying the direction of view, which is based upon the symmetry known (or thought) to be possessed by the particle.

The reconstruction method is straightforward in principle. The area of interest on the micrograph is converted to an array of optical density values by means of a computer-controlled film scanner (Arndt, Crowther & Mallett 1968). All further operations required for the reconstruction are performed by a digital computer. The digitized densities are transformed by computation into a set of Fourier amplitudes and phases. Each view of the particle provides a central section of Fourier space and the symmetry of the particle can be used to generate further central sections related to the first by the symmetry. By inserting data from views of the same particle in different orientations, or from different particles in independent orientations, and by making use of the symmetry, Fourier space is 'filled up' to enable the reconstruction to be carried out to a given degree of resolution. We consider later how to decide when the degree of filling up is sufficient for a valid reconstruction to be produced.

In order to be able to compute a correct Fourier inversion of the three-dimensional data so collected, the values of the transform must be available at regularly spaced points throughout its volume. Otherwise, an undistorted representation of the required density will not be obtained (formally, this happens because the result of a Fourier inversion of a sampled transform is the convolution of the required density with the transform of the sampling function). In general, however, the planes of collected data will contain relatively few of the regularly spaced transform points. To use them efficiently, the values of the transform at points where they happen to be available must somehow be interpolated to convert them to the values at the regularly spaced points required for the Fourier inversion.

We have developed several procedures, described in detail elsewhere (Crowther, DeRosier & Klug 1970), for carrying out this interpolation. Two types of grid system commend themselves. If normal Fourier inversion in Cartesian coordinates is used, the transform values must be available at points of a three-dimensional lattice and the Whittaker–Shannon formula is used to perform the interpolation. For Fourier–Bessel inversion in cylindrical polar coordinates the transform values are required on the grid formed by the intersection of the  $R$ ,  $\Phi$  and  $Z$  surfaces, in which case the interpolation is done by cylindrical expansion. According to the symmetry of the object, and the way in which the data have been collected, one or other of these representations may be particularly appropriate. In either case the grid spacings are determined by the limited extent of the original object. In the reconstructions described here we have used a cylindrical grid with Fourier–Bessel inversion, since this is computationally convenient.

## 3. INTERPOLATION BY CYLINDRICAL EXPANSION

We choose cylindrical polar coordinates  $(r, \phi, z)$  in the particle and  $(R, \Phi, Z)$  in the transform (figure 1). We expand the density  $\rho(r, \phi, z)$  in cylinder functions (Klug, Crick & Wyckoff 1958):

$$\rho(r, \phi, z) = \sum_{n=-\infty}^{\infty} \int_{-\infty}^{\infty} g_n(r, Z) \exp(in\phi) \exp(2\pi izZ) dZ. \quad (1)$$

The Fourier transform  $F(R, \Phi, Z)$  is then expressible in the form

$$F(R, \Phi, Z) = \sum_n G_n(R, Z) \exp(in(\Phi + \frac{1}{2}\pi)), \quad (2)$$

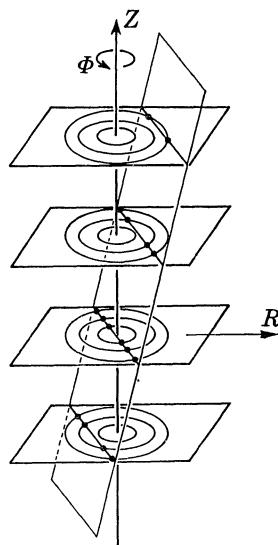


FIGURE 1. A cylindrical polar coordinate system is used to describe the transform, which is sampled on planes of constant  $Z$  and on annuli of constant  $R$  within each  $Z$  plane. It is shown schematically how a central plane corresponding to some view of the object cuts the various annuli.

where  $G_n(R, Z)$  is the Fourier-Bessel transform of  $g_n(r, Z)$

$$G_n(R, Z) = \int_0^{\infty} g_n(r, Z) J_n(2\pi Rr) 2\pi r dr, \quad (3)$$

and conversely

$$g_n(r, Z) = \int_0^{\infty} G_n(R, Z) J_n(2\pi Rr) 2\pi R dR. \quad (4)$$

We consider the three-dimensional transform to be sampled on a series of equally spaced planes of constant  $Z$  and each  $Z$  plane to be divided into a number of equally spaced concentric annuli, as shown schematically in figure 1. The form of equation (2) then implies that around an annulus of fixed  $R$  and  $Z$  the transform  $F$  is a known function of  $\Phi$ . In general some or all of the central sections of the transform computed from the given views of the particle will intersect any particular annulus at points  $\Phi_j$ , whose positions are determined by the angular parameters of the views. The transform values  $F_j$  at these points are then known. On each annulus we may write (2) as

$$F_j = \sum_n B_{jn} G_n, \quad (5)$$

where

$$B_{jn} = \exp(in(\Phi_j + \frac{1}{2}\pi)).$$

We have one set of linear equations (5) for each annulus.

On each annulus we may therefore attempt to solve equations (5) for the  $G_n(R, Z)$ . In this way we approximate each of the functions  $G_n(R, Z)$  by its values at a discrete set of equally spaced values in  $R$  and  $Z$ . The functions  $g_n(r, Z)$  can then be computed from (4), where the infinite integral is replaced by a finite summation over discrete points. The three-dimensional density is then computed by summing Fourier series (1), where again the infinite integral will be replaced by a finite summation over discrete  $Z$  values. Replacement of infinite integrals by finite summations is equivalent to truncating the Fourier series and fixes the resolution of the reconstruction. Inversion of the sampled, as opposed to the continuous, Fourier transform leads to a reconstruction in which the required density is repeated periodically with period equal to the inverse of the sample spacing. To avoid overlap of neighbouring images of the particle in the periodic reconstruction the sample spacing must therefore be smaller than the reciprocal of the diameter of the particle.

The number of  $G_n$  that can contribute on any annulus is fixed by the radius  $R$  of that annulus and by the radius of the particle. The Bessel function  $J_n(x)$  is effectively zero for  $0 < x < |n| - 2$ . It follows from (3) that the maximum order of Bessel function that can contribute on annulus  $R$  for a particle of radius  $a$  is  $n_{\max} \doteq (2\pi Ra + 2)$ .

A necessary condition for equations (5) to be soluble is that on each annulus there should be as many measured transform values  $F_j$  as unknowns  $G_n$ . However this is not a sufficient condition, since the points  $\Phi_j$  at which the transform is available may be very unfavourably spaced, so that the  $G_n$  are poorly determined.

In practice one must introduce extra views of the particle to give rather more data points than unknowns in each interpolation problem. We then solve these extended sets of equations by the method of least squares. We write (5) in matrix form as observational equations:

$$\mathbf{F} = \mathbf{B}\mathbf{G}. \quad (6)$$

We then form the normal equations:

$$\mathbf{B}^*\mathbf{F} = \mathbf{B}^*\mathbf{B}\mathbf{G},$$

which give a least squares solution of (6) as

$$\mathbf{G} = (\mathbf{B}^*\mathbf{B})^{-1}\mathbf{B}^*\mathbf{F}.$$

#### 4. THE NUMBER OF VIEWS REQUIRED

To produce a valid reconstruction to a given resolution, each set of normal equations corresponding to an annulus within the appropriate Fourier cut-off sphere must be soluble. We may investigate whether any of the normal matrices are singular by computing their eigenvalue spectra. Although in principle the normal matrix is invertible provided none of its eigenvalues is actually zero, in practice there is a lower limit for smallest eigenvalue, below which one cannot usefully invert the normal matrix. This is because solution of the equations by inversion of a normal matrix with very small eigenvalues effectively amplifies any errors in the data by a factor proportional to the mean inverse eigenvalue (Crowther, DeRosier & Klug 1970) and so may lead to a very inaccurate determination of the required  $G_n$ . For our problems we find that the method produces consistent solutions if the mean inverse eigenvalue of every normal matrix is less than unity. In practice this means that on most annuli the mean inverse eigenvalue is considerably less than unity, as we shall see later.

The number of views that must be included in order to satisfy this condition depends on which views are available and also on the size of the object and the degree of resolution desired, since these fix the number of terms to be included in the Fourier inversion and therefore the number of unknowns in each least squares problem. It also depends on the symmetry of the object, since this may be used to reduce the size of the least squares problems by a suitable choice of coordinate system. We give an example of this use of symmetry later. Finally the number of views required depends on which method of interpolation is used. The relative power of various interpolation schemes is assessed elsewhere (Crowther, DeRosier & Klug 1970). It is shown there that although Whittaker–Shannon interpolation in a Cartesian system uses data more efficiently than the cylindrical expansion scheme described here, the computational convenience of the latter more than outweighs this at present.

##### 5. REFINEMENT OF PARTICLE ORIENTATION AND ORIGIN POSITION

To use the symmetry of the spherical viruses and also to relate different particles, we must know the orientation relative to the symmetry axes of any view that we propose to include in the reconstruction. This can be determined by a method which depends on the existence of a set of pairs of ‘common lines’ in the two-dimensional transform of any view of a symmetrical particle. These arise as follows. An observed section of the transform intersects an identical symmetry related section in a line, along which the transform must have the same value in both sections. The common line lies in the original section. However, regarded as lying in the symmetry related section it must have been generated by the symmetry operation from some other line in the original section. We therefore have a pair of lines in the original transform plane along which the transform must have identical values. A similar pair of lines will be generated by each possible choice of pairs of symmetry operations. The angular positions of these lines are dependent on the orientation of the particle.

Since the disposition of the various pairs of common lines in the transform of a particle cannot be recognized directly it is necessary to search for them computationally. We compare the differences in the observed values of the transform along the set of common lines corresponding to a particular choice of orientation parameters. The minimum value of the sum of these differences will occur when the angular parameters correspond to the true orientation of the particle. The orientation of an unknown view of a particle can be determined by searching a complete asymmetric unit of rotation space. The search can be restricted to a small range if a preliminary estimate of the orientation of the view is available (from, say, comparison of the image with a trial model), in which case the method serves for refinement.

The common lines may also be used to determine the translational position of the centre of the particle, defined as the projected point of intersection of all the symmetry axes. It is vital that the phases of the various two-dimensional Fourier transforms and of the three-dimensional Fourier transform should all be referred to this common point as origin. For a given orientation the positions of the common lines are fixed and changes in the position of the phase origin affect only the phases of the transform. Although in theory one ought to perform a five-dimensional search for three angles and two translations simultaneously, in practice it is possible to choose the initial phase origin close enough to the particle centre for the phase errors introduced to have little effect on the determination of the orientation. Thus the orientation is determined by a three-dimensional search using phases computed relative to a slightly incorrect phase origin.

Taking the orientation so determined one does a two-dimensional search to refine the position of the phase origin. If a new angular search is now made using transform phases computed relative to the refined phase origin, the value of the sum of differences at the minimum will be smaller, although in general the position of the minimum will be unaltered. The computational advantages of splitting the search in this way are considerable.

The value of the sum of differences at the point given by the program for the solution of the five-dimensional search provides a measure of the degree of preservation of the icosahedral symmetry in the particular particle whose image is being investigated. Since we can compute the residual to various limits in Fourier space, it is possible to decide to what degree of resolution the details in a particle image are related by icosahedral symmetry. Clearly, data should be included only if they show some degree of icosahedral correlation: beyond this limit any transform data are contributing only noise to the final reconstruction.

We have so far considered common lines occurring in the transform of a single image. If, however, we have two independent views coming from two particles in different orientations, the transforms of these two images must also contain a set of pairs of common lines, where now one member of each pair lies in one transform while the other lies in the other transform. It would clearly be possible to use these 'cross common lines' to determine the relative orientation of the two views. However, it is more useful in this particular problem to determine the orientation of each view independently by self-refinement in the way already described and then to use the cross common lines to ensure that the two transforms are on the same linear scale and that the magnitudes of the two transforms along the common lines agree as well as possible. We fit an overall radial scale factor and an amplitude scale factor as a function of radius. The latter is analogous to a crystallographic temperature factor and ensures that when Fourier components corresponding to a particular spatial frequency are obtained from different images, they are combined with the correct relative weights.

The cross common lines are also used to ensure that the various images are combined with a consistent handedness. Any one image may derive from a projection either of a right-handed particle or of a left-handed particle in the same direction. The only difference in the two cases and one that is not detectable without tilting, is that the azimuthal orientation of the image in its own plane differs by  $180^\circ$ . Once one of these two possible orientations has been arbitrarily assigned to an image possessing a noncentrosymmetric component, the handedness of the reconstruction is fixed. As assignment of orientation to a further view consistent with this choice of hand can be made, by examination of the two sets of common lines arising from the first view and from the two possible orientations of the added view and by choice of that orientation which gives the lower residual. Although this leads to a consistent hand, the correct absolute hand must be determined by tilting experiments (Klug & Finch 1968).

## 6. COMPUTATIONAL PROCEDURE

In neither cylindrical nor Cartesian coordinates is it possible to express in the underlying mathematical representation the complete 532-point group symmetry of the icosahedral viruses. In cylindrical coordinates the most economical method is to choose the polar axis to coincide with a fivefold axis of the particle, so that only those  $G_n(R, Z)$  for which  $n$  is a multiple of 5 need be included. If in addition we choose the origin of  $\Phi$  to lie midway between two of the twofold axes normal to this fivefold axis, the interpolation equations can be separated into real

## THREE-DIMENSIONAL RECONSTRUCTION OF VIRUSES 227

and imaginary parts, in a way convenient for computation (Crowther, DeRosier & Klug 1970). We have in this way chosen a representation for the problem which possesses 522 symmetry. The additional symmetry of the 532-point group must be used by explicitly generating from any given view those icosahedrally related planes which are not already implicitly included

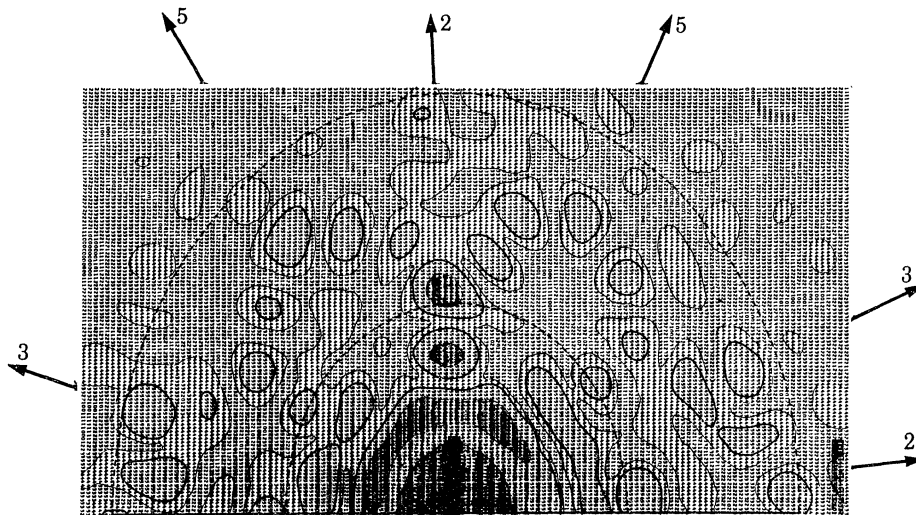


FIGURE 2. Part of a two-dimensional Fourier transform of a particle of tomato bushy stunt virus viewed along a twofold axis (particle B in figure 4). The map, which shows  $\log_2 |F|$ , is a photograph of contoured computer output and is distorted because of unequal line printer spacings in the two principal directions. The inner and outer dotted semicircles indicate Fourier spacings of approximately 7 and 3.5 nm respectively. Those icosahedral symmetry axes lying in the plane of the transform are indicated and, as expected (Caspar 1956), there tend to be strong spikes in these directions.

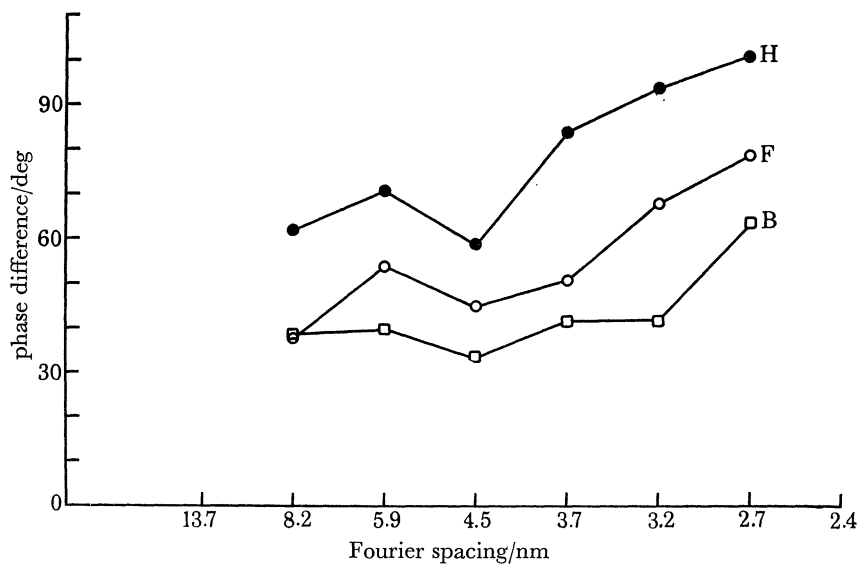


FIGURE 3. Plots for tomato bushy stunt virus particles B, F and H (figure 4) showing for each particle how the common lines residual, computed for the orientation and position parameters corresponding to the minimum value when using all the data, behaves when computed from data lying in a series of bands of increasing radius in the transform. For convenience the residual is expressed as a mean difference in the phase of the transform along the pairs of common lines and a value close to  $90^\circ$  indicates no icosahedral correlation. B and F are relatively good particles while H is rather poor.



within the 522 symmetry of the representation. The final reconstruction must have exact 522 symmetry since only functions having this symmetry are admitted. It will possess 532 symmetry only if the images included really do arise from an object with 532 symmetry and if their orientations have been correctly determined. This provides an added check on the results.

We thus adopt the following procedure. A number of particles are densitometered and their two-dimensional Fourier transforms are computed choosing a phase origin as close as possible to the centre of each particle. Fast Fourier transform methods are used (Cooley & Tukey 1965), as implemented by DeRosier & Moore (1970). Figure 2 shows an example of the amplitude part of such a transform obtained from a particle of tomato bushy stunt virus. The orientation of each particle and the position of its centre are determined accurately by the common lines technique, which also enables us to estimate how well the icosahedral symmetry has been preserved. Figure 3 shows for a number of tomato bushy stunt virus particles how the common lines residual at the point with minimum value behaves as a function of increasing radius in the transform. The results are plotted in terms of mean phase differences, where a value of  $90^\circ$  indicates zero icosahedral correlation. The cross common lines are then used to put the various images on the same scale and to choose a consistent hand.

Taking the best particles, as judged by their common lines residuals, we compute where each transform plane, together with the symmetry related planes, intersects the various annuli and extract the information required for setting up the normal equations. We then combine the information from a number of particles and attempt to solve the normal equations on each annulus for the  $G_n(R, Z)$ . We go on including extra views until the normal equations become soluble on every annulus, as judged by their eigenvalues.

Typically in our problems we must include three or four views to satisfy the criterion, given in § 4, that the mean inverse eigenvalue of each normal matrix should be less than one. Specifically for tomato bushy stunt virus with diameter 32 nm, if we make the separation of the  $Z$  planes and the annuli within each  $Z$  plane both equal to  $\frac{1}{64} \text{ nm}^{-1}$  and solve out to a Fourier cut-off of 2.3 nm there are 613 annuli within the cut-off sphere. On each annulus we solve two sets of normal equations, one for real parts and one for imaginary parts. When we include the four particles B, D, F, G (see figure 4, plate 43), whose orientations are given by spherical polar angles  $(90^\circ, 0^\circ)$ ,  $(94^\circ, 76.5^\circ)$ ,  $(88.5^\circ, 81^\circ)$  and  $(95^\circ, 15^\circ)$  and which thus span the asymmetric unit in Fourier space fairly well, of the 1226 sets of equations 944 have a mean inverse eigenvalue between  $10^{-2}$  and  $10^{-1}$  and the remaining 282 have a mean inverse eigenvalue between  $10^{-1}$  and 1.

Having solved the normal equations we convert each  $G_n(R, Z)$  to the corresponding  $g_n(r, Z)$  by a Fourier-Bessel transform (4) and then produce the three-dimensional density map by summing Fourier series (1). The results are plotted section by section either as contour or density maps, using a general plotting program (Gossling 1967).

#### 7. APPLICATION TO TOMATO BUSHY STUNT VIRUS

Tomato bushy stunt virus (TBSV) has a maximum diameter of 33 nm and a spherically averaged diameter of 31 nm (Review by Klug & Caspar 1960). The major component of the coat protein is arranged on a  $T = 3$  icosahedral surface lattice, the 180 quasi-equivalent structural units being clustered in dimers to form ninety morphological units (Finch, Klug & Leberman 1970). Of these ninety morphological units, thirty lie on the strict twofold axes of the

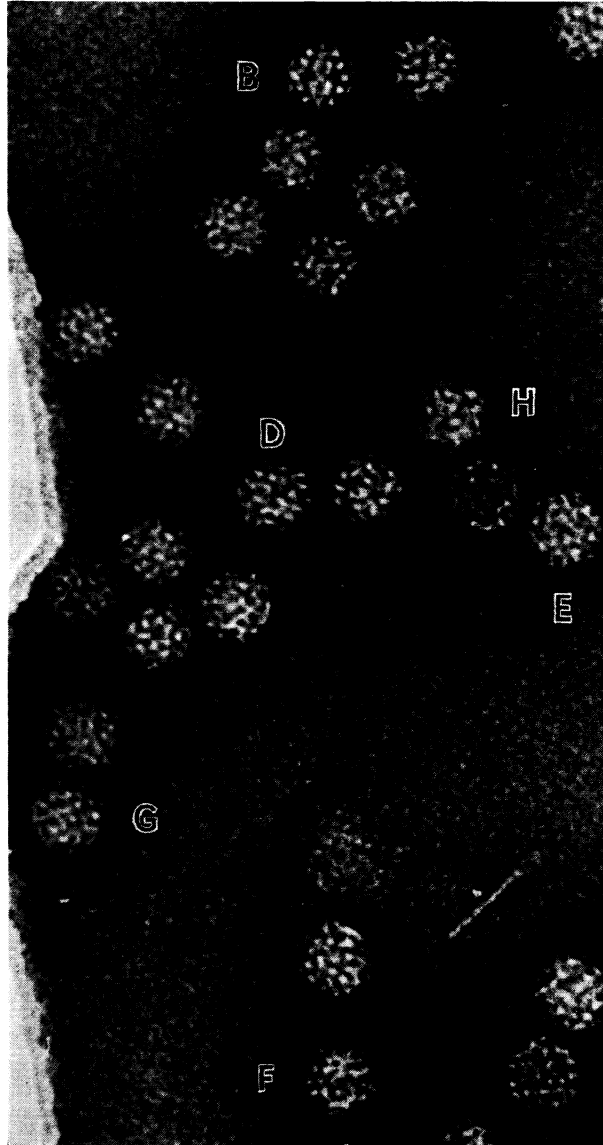


FIGURE 4. A field of particles of tomato bushy stunt virus embedded in negative stain over a hole in the substrate. Some of the particles used in the reconstruction are indicated.

(Facing p. 228)

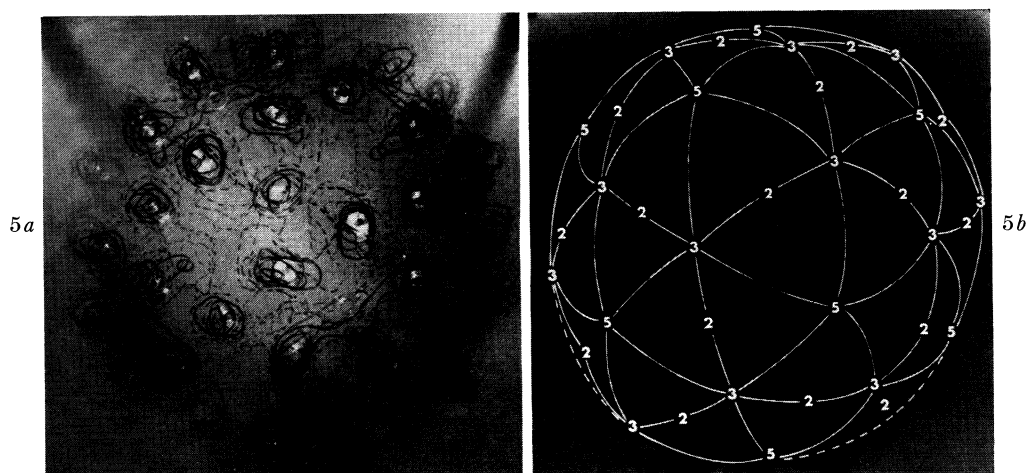


FIGURE 5. (a) Contour map of a reconstruction of tomato bushy stunt virus. (b) The same map (photographed using different illumination) with the  $T = 3$  surface lattice (Caspar & Klug 1962) superimposed. Contours indicate the absence of stain. The principal morphological units lying on the strict and local twofold axes of the lattice are indicated by nuts while the subsidiary morphological units at the fivefold positions are marked by washers.

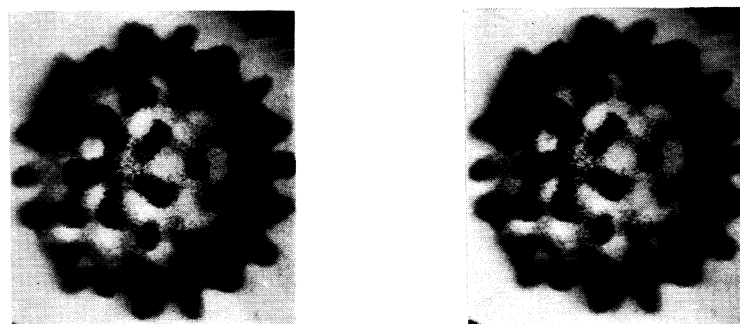


FIGURE 6. A stereo-pair of the top half of a density plot of the TBSV reconstruction, in which high density indicates the absence of stain. For full effect this diagram must be viewed with a stereoscopic viewer.

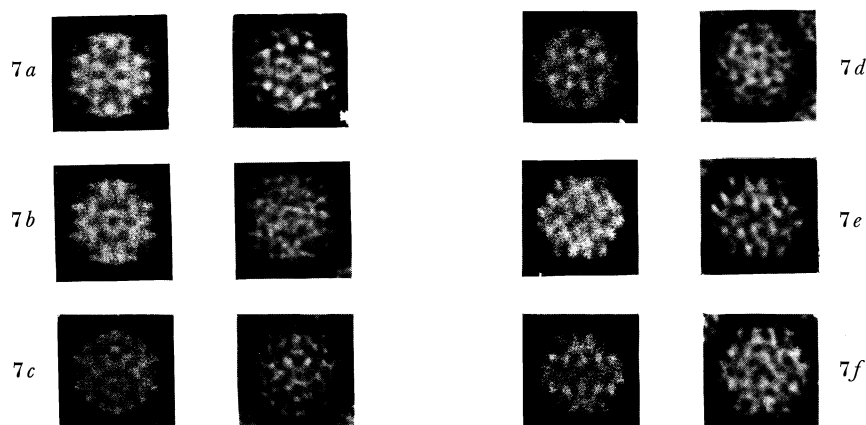


FIGURE 7. Comparison of projections in different directions of the reconstructed density with images of virus particles in the corresponding orientations. The good agreement between the two sets of pictures extends to fine detail, even though the relative weights of some features are not quite correct since the reconstruction was not 'embedded in negative stain' before computing its projections. The spherical polar angles specifying the views are: (a)  $(90^\circ, 0^\circ)$  particle B; (b)  $(90^\circ, 10^\circ)$ ; (c)  $(90^\circ, 25^\circ)$ ; (d)  $(92^\circ, 48^\circ)$ ; (e)  $(94^\circ, 76.5^\circ)$  particle D; (f)  $(92^\circ, 80^\circ)$  particle E.

surface lattice, and sixty on the local twofold axes. These sixty are arranged in twelve rings of five, whose centres partially exclude the stain, indicating the presence of protein.

Until recently, no simple correlation could be made between the morphology and the published physico-chemical data for this virus or for the very similar turnip crinkle virus (Harrison 1967; Finch *et al.* 1970). Recent work on both viruses has established the molecular mass of the major protein subunit as about 40 000 (Butler 1970; Weber, Rosenbusch & Harrison 1970), consistent with a total of 180 in the particle. Each of the ninety morphological units would therefore correspond to a pair of protein subunits, in agreement with the expected symmetry. Butler's work has also revealed the presence of a minor protein component in a suitable amount to account for the matter observed at the fivefold positions of the surface lattice.

For the reconstruction we chose a particularly favourable micrograph, where particles are embedded in negative stain over a hole in the carbon substrate, as shown in figure 4. Experimental details of virus preparation and electron microscopy are given by Finch *et al.* (1970). The particles in this field have shrunk by about 10% from their normal diameter in solution, but this shrinkage is in many cases isometric and preserves the icosahedral symmetry, as judged by the common lines technique. Icosahedral correlation appears to extend to at least 2.5 nm for good particles (figure 3), showing that detailed symmetry is preserved almost to the limiting resolution of the negative staining technique.

Four of the best particles (B, D, F, G) indicated in figure 4 were combined including data out to a cut-off of 2.3 nm. The reconstruction is shown as a contour map in figure 5, plate 44, and as a stereo-pair of a density plot in figure 6, plate 44. Figure 7, plate 44, shows comparisons between images from electron micrographs and projections of the reconstructed density in the corresponding directions. The agreement between the two sets is remarkably good, particularly as the reconstructed particle has not been 'embedded in negative stain' before projecting, so that the relative weights of the various parts of the projections may not be quite correct.

As expected, the main concentrations of density in the reconstruction are on the strict and local twofold axes of the surface lattice so that the morphological units are presumably dimers. These morphological units are arranged in rings of six and five, and there is also density at the centres of the rings of five, giving them the appearance of five-pointed stars. We cannot yet tell whether this density arises from the shape of the principal structure unit itself or from the minor protein component mentioned above. Density also appears in the rings of six, but at a much smaller radius, and probably represents a coming together of the inner parts of the structure units, possibly in association with the nucleic acid.

The reconstruction also shows that the dimers on the local twofold axes (i.e. those dimers forming rings of five) lie at a greater radius than those dimers on strict twofold axes, so that the five-pointed 'stars' stand out from the surface. This effect also shows itself as a puckering of the rings of six, which is visible in figure 6. We estimate the difference in radius to be about 1 nm. This observation confirms the results of X-ray crystallographic studies of TBSV (Harrison 1967).

Finally there is a marked absence of density at the local threefold positions, that is approximately between the points of the 'star', indicating deep penetration of stain into these places. This suggests that the nucleic acid is folded within the particle in such a way as to avoid these regions.

## 8. CONCLUSIONS

The reconstruction described here demonstrates that it is in practice possible to combine data from a number of different particles. Using fast Fourier transform methods for computing the two-dimensional transforms, the total time needed to compute a reconstruction from four views starting from raw densitometer data and ending with a computer display suitable for contouring is about  $1\frac{3}{4}$  h on an IBM 360/44 computer. Although in the case of spherical viruses with their high symmetry the number of views needed is small, there is in principle no reason why the method should not be extended to systems with lower symmetry for which many more views must be combined to achieve the same degree of resolution. For successful implementation it will be necessary to improve methods of specimen preservation during a tilting series in the electron microscope and to use larger and faster computers to process the large volume of data that will be needed.

I am grateful to Mrs Linda Amos for writing computer programs to carry out the procedures described in this paper. The electron micrographs were kindly supplied by Dr J. T. Finch.

## REFERENCES (Crowther)

- Arndt, U. W., Crowther, R. A. & Mallett, J. F. W. 1968 *J. scient. Instrum.* (2), **1**, 510.  
 Butler, P. J. G. 1970 *J. molec. Biol.* **52**, 589.  
 Caspar, D. L. D. 1956 *Nature, Lond.* **177**, 475.  
 Caspar, D. L. D. & Klug, A. 1962 *Cold Spring Harbor Symp. quant. Biol.* **27**, 1.  
 Cooley, J. W. & Tukey, J. W. 1965 *Maths. Computation* **19**, 297.  
 Crowther, R. A., Amos, L. A., Finch, J. T., DeRosier, D. J. & Klug, A. 1970 *Nature, Lond.* **226**, 421.  
 Crowther, R. A., DeRosier, D. J. & Klug, A. 1970 *Proc. Roy. Soc. Lond. A* **317**, 319.  
 DeRosier, D. J. & Klug, A. 1968 *Nature, Lond.* **217**, 130.  
 DeRosier, D. J. & Moore, P. B. 1970 *J. molec. Biol.* **52**, 355.  
 Finch, J. T. & Gibbs, A. J. 1970 *J. Gen. Virol.* **6**, 141.  
 Finch, J. T., Klug, A. & Leberman, R. 1970 *J. molec. Biol.* **50**, 215.  
 Gossling, T. H. 1967 *Acta Crystallogr.* **22**, 465.  
 Harrison, S. C. 1967 Ph.D. Thesis, Harvard University.  
 Klug, A. & Caspar, D. L. D. 1960 *Adv. Virus Res.* **7**, 225.  
 Klug, A., Crick, F. H. C. & Wyckoff, H. W. 1958 *Acta Crystallogr.* **11**, 199.  
 Klug, A. & Finch, J. T. 1968 *J. molec. Biol.* **31**, 1.  
 Moore, P. B., Huxley, H. E. & DeRosier, D. J. 1970 *J. molec. Biol.* **50**, 279.  
 Weber, K., Rosenbusch, J. & Harrison, S. C. 1970 *Virology*, **41**, 763.

Downloaded from [rstb.royalsocietypublishing.org](http://rstb.royalsocietypublishing.org)

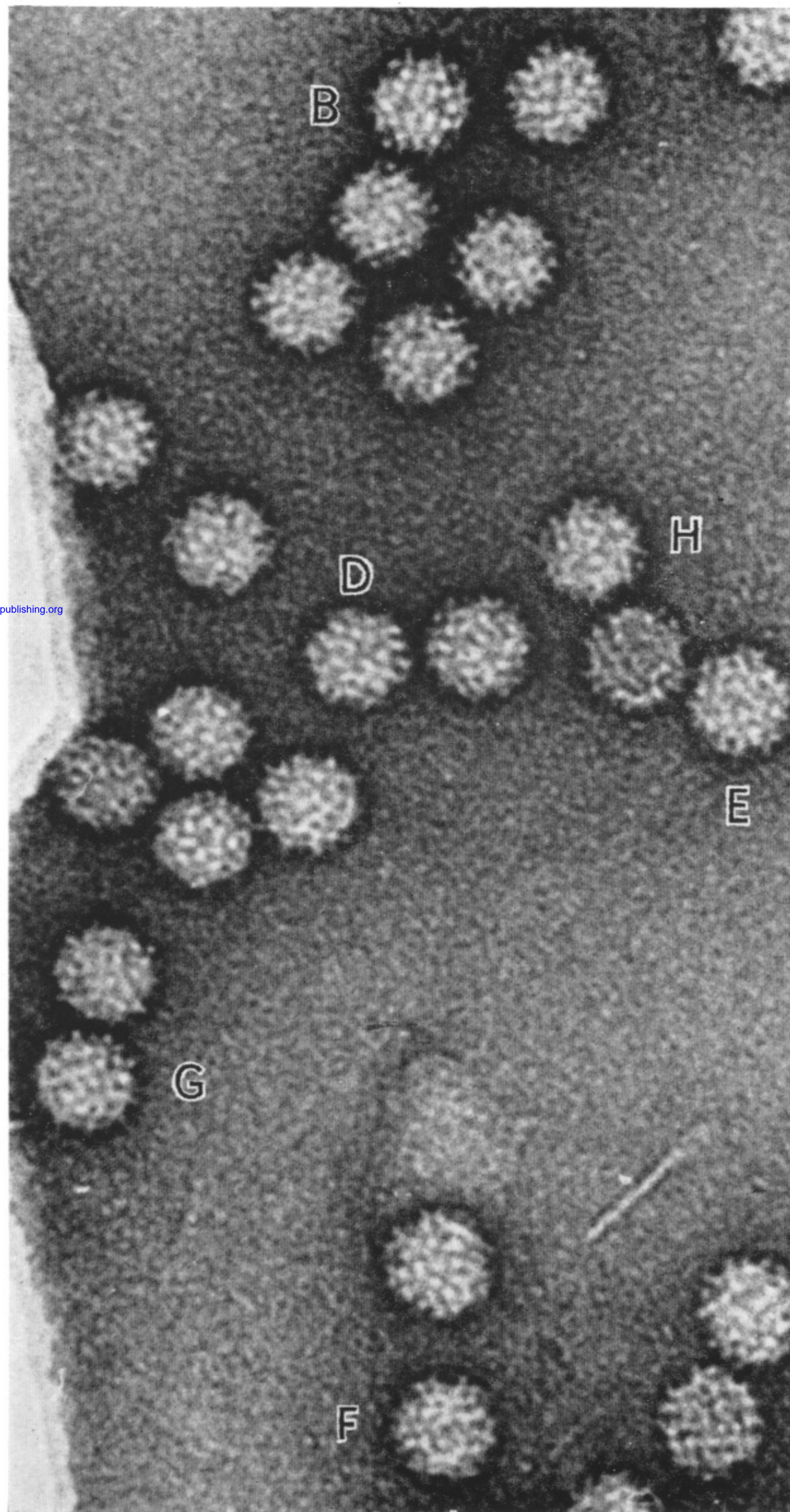
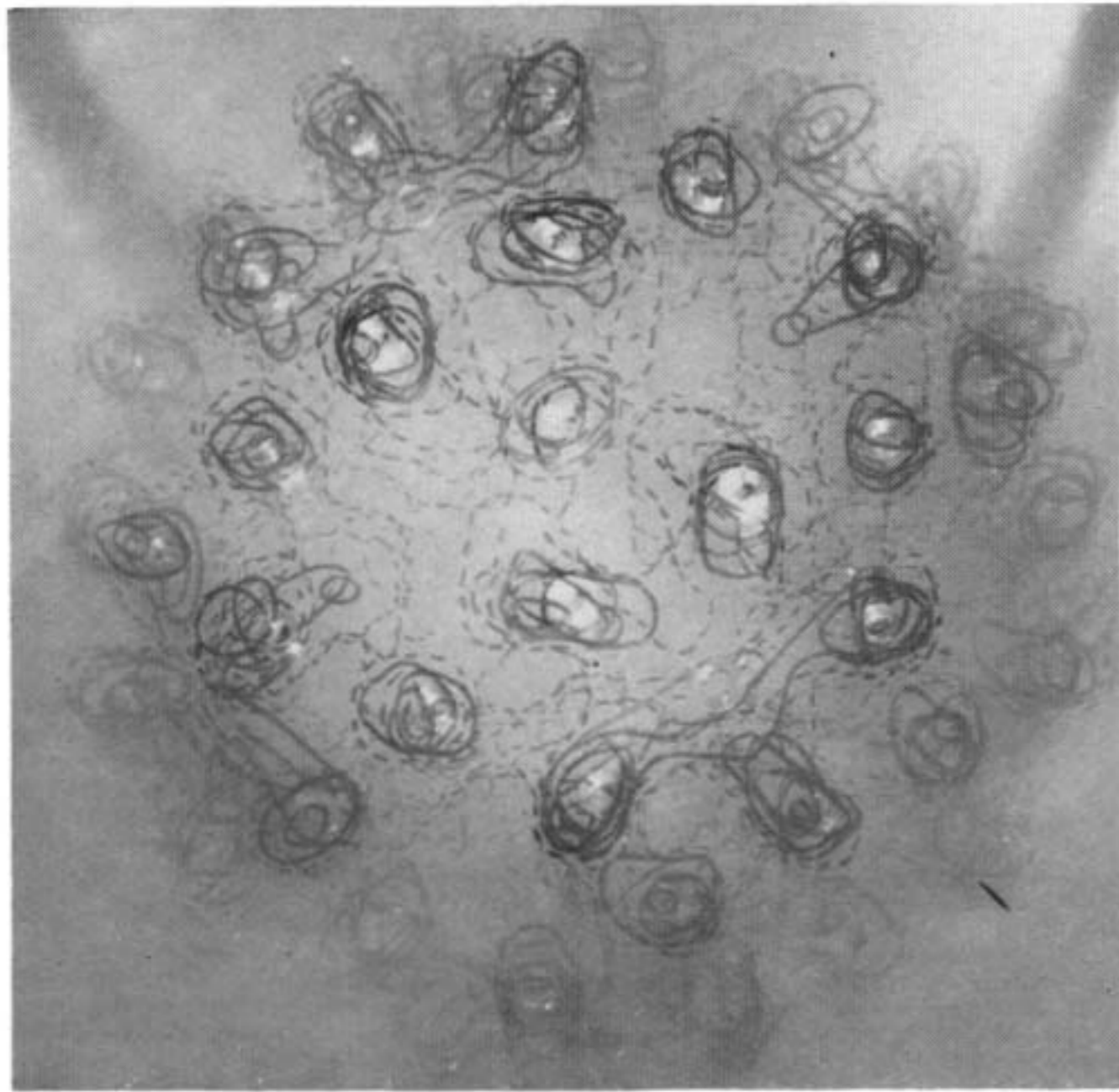


FIGURE 4. A field of particles of tomato bushy stunt virus embedded in negative stain over a hole in the substrate. Some of the particles used in the reconstruction are indicated.

5a



5b

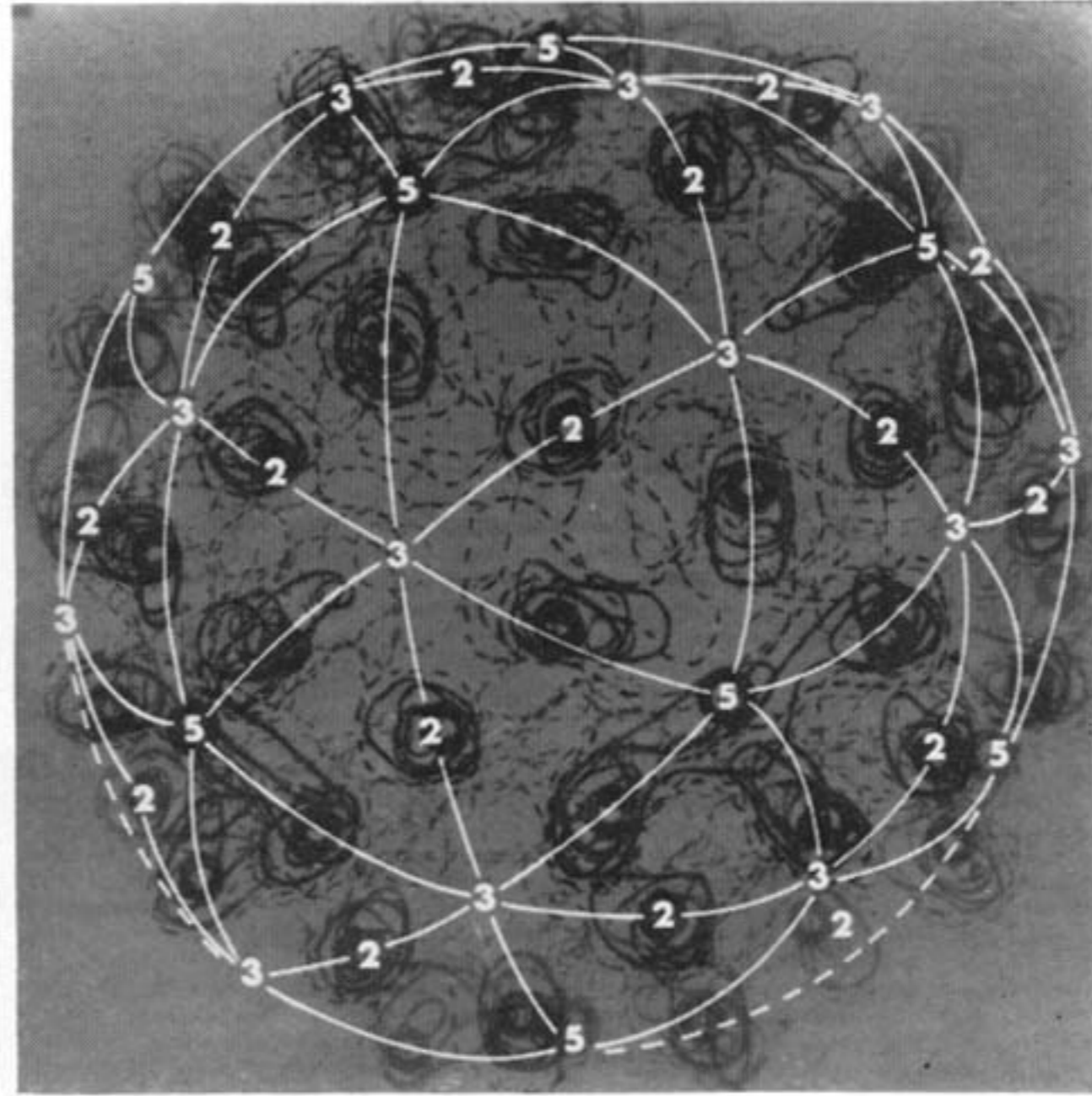


FIGURE 5. (a) Contour map of a reconstruction of tomato bushy stunt virus. (b) The same map (photographed using different illumination) with the  $T = 3$  surface lattice (Caspar & Klug 1962) superimposed. Contours indicate the absence of stain. The principal morphological units lying on the strict and local twofold axes of the lattice are indicated by nuts while the subsidiary morphological units at the fivefold positions are marked by washers.

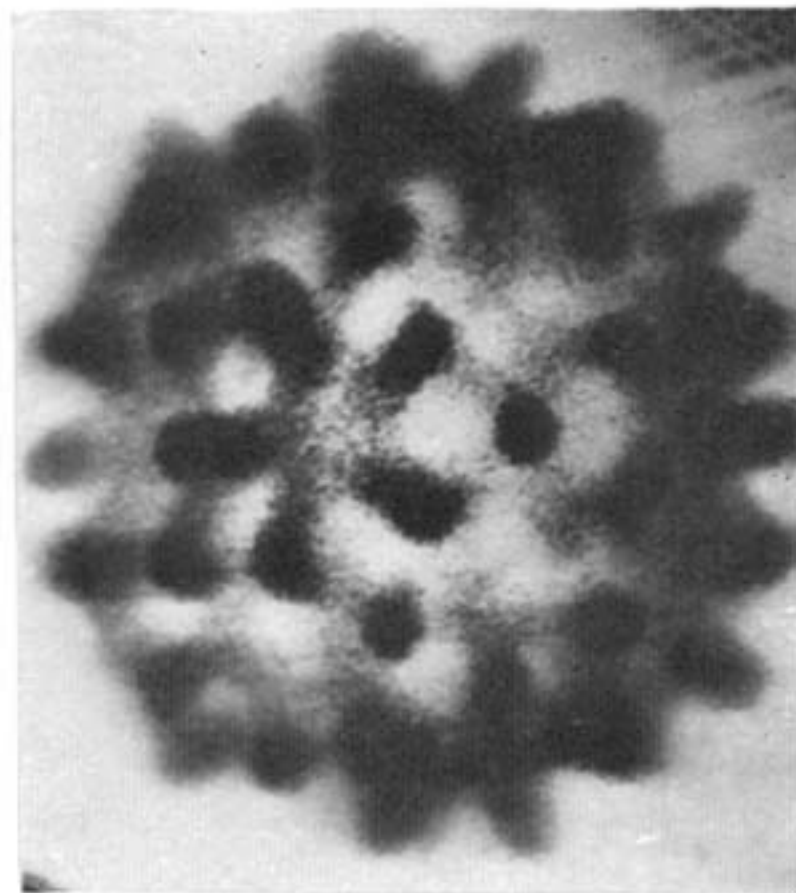
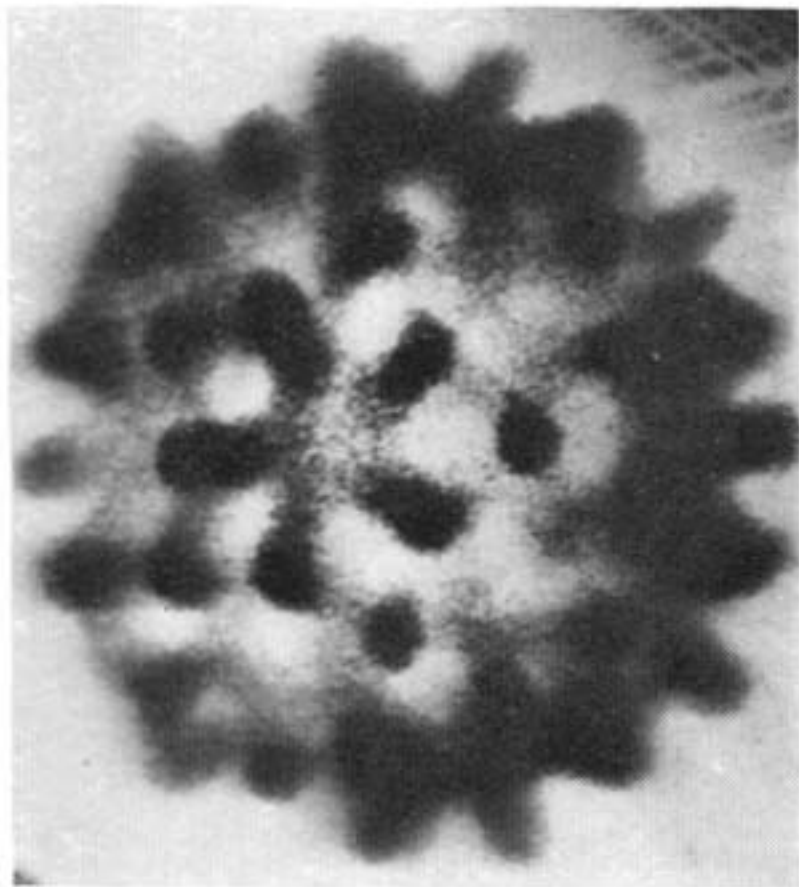


FIGURE 6. A stereo-pair of the top half of a density plot of the TBSV reconstruction, in which high density indicates the absence of stain. For full effect this diagram must be viewed with a stereoscopic viewer.



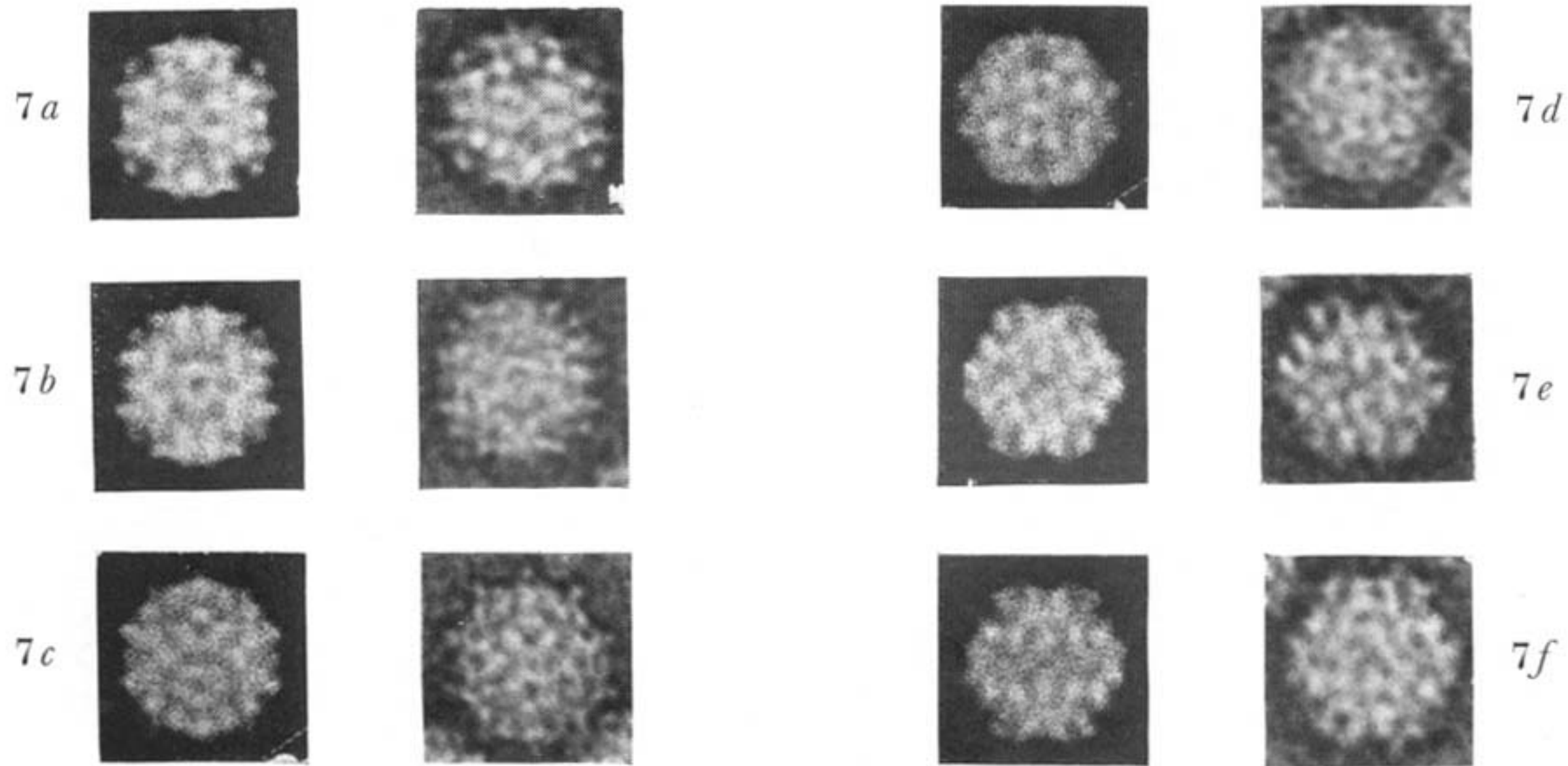


FIGURE 7. Comparison of projections in different directions of the reconstructed density with images of virus particles in the corresponding orientations. The good agreement between the two sets of pictures extends to fine detail, even though the relative weights of some features are not quite correct since the reconstruction was not 'embedded in negative stain' before computing its projections. The spherical polar angles specifying the views are: (a)  $(90^\circ, 0^\circ)$  particle B; (b)  $(90^\circ, 10^\circ)$ ; (c)  $(90^\circ, 25^\circ)$ ; (d)  $(92^\circ, 48^\circ)$ ; (e)  $(94^\circ, 76.5^\circ)$  particle D; (f)  $(92^\circ, 80^\circ)$  particle E.